JOURNAL OF APPLIED ELECTROCHEMISTRY 22 (1992) 471–477

# Transition metal-based cathodes for hydrogen evolution in alkaline solution: electrocatalysis on nickel-based ternary electrolytic codeposits

I. ARUL RAJ, K. I. VASU

*Central Electrochemical Research Institute, Karaikudi 623006, India*

Received 3 July 1991; revised 1 October 1991

Nickel–molybdenum–iron, nickel–molybdenum–copper, nickel–molybdenum–zinc, nickel–molybdenum–cobalt, nickel–molybdenum–tungsten and nickel–molybdenum–chromium ternary codeposits, obtained through electrodeposition on mild steel strips have been characterized with the objective of qualitatively comparing and assessing their electrocatalytic activities as hydrogen electrodes in alkaline solution. It has been concluded that their electrocatalytic effects for the hydrogen evolution reaction (h.e.r.) rank in the following order: Ni–Mo–Fe > Ni–Mo–Cu > Ni–Mo–Zn > Ni–Mo–Co ~ Ni–Mo–W > Ni–Mo–Cr > Ni-plated steel. Further investigations on these electrocatalysts have revealed that the cathodic overpotential contribution to the electrolysis voltage can be brought down by 0.3 V when compared with conventional steel cathodes. The best and most stable hydrogen evolving cathode of these, namely Ni–Mo–Fe, exhibited an overpotential of about 0.187 V for over 1500 h of continuous electrolysis in 6 M KOH at 300 mA $cm^{-2}$ and 353 K. The salient features of the codeposits, such as physical characteristics, chemical composition, current–potential behaviour and the varying effects of the catalytic activation method were analysed with a view to correlating the micro-structural characteristics of the coatings with the hydrogen adsorption process. The stability under open circuit conditions, the tolerance to electrochemical corrosion and the long term stability of Ni–Mo–Fe codeposit cathodes were very encouraging. An attempt to identify the pathway for the h.e.r. on these codeposit cathodes was made, in view of the electrochemical parameters obtained experimentally.

## 1. Introduction

In continuing our search for electrocatalytic materials for hydrogen electrodes based on transition metals in alkaline solution [1–3] along with various other groups [4–9], we report here the results of experiments on some ternary electrolytic codeposits based on nickel–molybdenum–iron/copper/zinc/cobalt/tungsten/chromium, as hydrogen evolving cathodes in alkaline solution. A discussion on the physical characteristics of the codeposits, the electrochemical parameters for the h.e.r. on these codeposit cathodes and the results of life tests by simulation experiments has been included.

## 2. Experimental details

### 2.1. *Pretreatment and deposition processes*

Mild steel foils of composition 0.06%C, 0.04%Si, 0.3%Mn, 0.002%P, 0.003%Cr, 0.008%Ni and 0.006%Mo were cut into 20 cm × 5 cm rectangular strips. The shearing edges of the strips were machined to a smooth finish. The pretreatment procedure involved initial mechanical surface polishing to a mirror finish using fine emery cloth (John Oakey) followed by sand blasting. The surfaces were washed, dried and thoroughly degreased with acetone followed by washing in triple distilled water. This was followed by cathodic cleaning in an alkaline bath containing sodium hydroxide 40%, sodium silicate 10% and sodium phosphate 10% at 353 K and 100 mA $cm^{-2}$ current density for 3 min. This was followed by anodic, and again cathodic, cleaning under similar conditions. Before electrodeposition, each substrate was washed thoroughly using triple distilled water.

The deposition processes were carried out using a geometric area of 130 $cm^2$ (total area), masking the rest with alkali resistant epoxy resin under galvanostatic steady state conditions, using two thin rectangular graphite strips as anodes, on both sides of the cathodes. The anodes were contained in Nylon bags. The details of the bath and the deposition conditions are presented in Table 1. Each codeposition was carried out on three similar substrates under identical conditions.

### 2.2. *SEM, XRD and AAS experiments*

The surface microstructures of the alloy coatings were investigated using scanning electron microscopy (SEM JEOL JSM 35 CF). The chemical composition of each codeposit was obtained by using the EPMA technique. The electron beam was fixed corresponding

0021-891X/92 

*Table 1. Bath characteristics and operating conditions for electrolytic codeposition*

| *Ni–Mo–Fe* | | *Ni–Mo–Cu* | | *Ni–Mo–Zn* | |
|---|---|---|---|---|---|
| *Parameters* | *Values* | *Parameters* | *Values* | *Parameters* | *Values* |
| $NiSO_4 \cdot 6H_2O$ | 85 g dm$^{-3}$ | $NiSO_4 \cdot 6H_2O$ | 85 g dm$^{-3}$ | $NiSO_4 \cdot 6H_2O$ | 150 g dm$^{-3}$ |
| $Na_2MoO_4 \cdot 2H_2O$ | 10 g dm$^{-3}$ | $Na_2MoO_4 \cdot 2H_2O$ | 10 g dm$^{-3}$ | $ZnSO_4 \cdot 7H_2O$ | 40 g dm$^{-3}$ |
| $K_3C_6H_5O_7 \cdot H_2O$ | 60 g dm$^{-3}$ | $K_3C_6H_5O_7 \cdot H_2O$ | 60 g dm$^{-3}$ | $Na_2MoO_4 \cdot 2H_2O$ | 20 g dm$^{-3}$ |
| $FeSO_4 \cdot 7H_2O$ | 10 g dm$^{-3}$ | $CuSO_4 \cdot 5H_2O$ | 10 g dm$^{-3}$ | $NH_4Cl$ | 30 g dm$^{-3}$ |
| $Na_2CO_3$ | Excess | $Na_2CO_3$ | Excess | $CH_3COONa$ | 30 g dm$^{-3}$ |
| pH | 10 | pH | 10–11 | $H_3BO_3$ | 15 g dm$^{-3}$ |
| Temperature | 301 K | Temperature | 301 K | pH | 5.5–6.5 |
| Current density | 10 mA cm$^{-2}$ | Current density | 10 mA cm$^{-2}$ | Temperature | 333 K |
| Duration | 90 min | Duration | 90 min | Current density | 5 mA cm$^{-2}$ |
| Agitation | 250 r.p.m. | Agitation | 250 r.p.m. | Duration | 90 min |
| Deposit weight | 3.5 mg cm$^{-2}$ | Deposit weight | 5.2 mg cm$^{-2}$ | Deposit thickness | 7.5 $\mu$m |
| Deposit thickness | 4.0 $\mu$m | Deposit thickness | 5.6 $\mu$m | Deposit colour | Dull white |
| Deposit colour | Dull grey | Deposit colour | Brownish grey | Adhesion | Very good |
| Adhesion | Very good | Adhesion | Very good | | |

| *Ni–Mo–W* | | *Ni–Mo–Co* | | *Ni–Mo–Cr* | |
|---|---|---|---|---|---|
| *Parameters* | *Values* | *Parameters* | *Values* | *Parameters* | *Values* |
| $NiSO_4 \cdot 6H_2O$ | 85 g dm$^{-3}$ | $NiSO_4 \cdot 6H_2O$ | 85 g dm$^{-3}$ | $NiSO_4 \cdot 6H_2O$ | 85 g dm$^{-3}$ |
| $Na_2MoO_4 \cdot 2H_2O$ | 10 g dm$^{-3}$ | $Na_2MoO_4 \cdot 2H_2O$ | 10 g dm$^{-3}$ | $Na_2MoO_4 \cdot 2H_2O$ | 10 g dm$^{-3}$ |
| $Na_2WO_4 \cdot 2H_2O$ | 10 g dm$^{-3}$ | $K_3C_6H_5O_7 \cdot H_2O$ | 60 g dm$^{-3}$ | $K_3C_6H_5O_7 \cdot H_2O$ | 60 g dm$^{-3}$ |
| $K_3C_6H_5O_7 \cdot H_2O$ | 60 g dm$^{-3}$ | $Co(NO_3)_2 \cdot 6H_2O$ | 10 g dm$^{-3}$ | $CrO_3$(Dil $\cdot$ $HNO_3$) | 20 g dm$^{-3}$ |
| $Na_2CO_3$ | Excess | $Na_2CO_3$ | Excess | $Na_2CO_3$ | Excess |
| pH | 10.5 | pH | 10 | pH | 10.5 |
| Temperature | 301 K | Temperature | 301 K | Temperature | 301 K |
| Current density | 10 mA cm$^{-2}$ | Current density | 10 mA cm$^{-2}$ | Current density | 10 mA cm$^{-2}$ |
| Duration | 90 min | Duration | 90 min | Duration | 90 min |
| Agitation | 250 r.p.m. | Agitation | 250 r.p.m. | Agitation | 250 r.p.m. |
| Deposit weight | 3.5 mg cm$^{-2}$ | Deposit weight | 7.5 mg cm$^{-2}$ | Deposit weight | 5.5 mg cm$^{-2}$ |
| Deposit thickness | 4.5 $\mu$m | Deposit thickness | 8–12 $\mu$m | Deposit thickness | 7–9 $\mu$m |
| Deposit colour | Black | Deposit colour | Black | Deposit colour | Bright white |
| Adhesion | Good | Adhesion | Good | Adhesion | Very good |

to the wavelength of the metals at a selected point on the surface and also scanned over a wide area to record the degree of homogeneity from the EPMA spectrum.

The XRD (X-ray diffraction) studies were carried out with cobalt-$K_\alpha$ radiation (25 mA, 35 kV) in the range of 10 Hz, at a scan rate of 2 min only for the Ni–Mo–Fe codeposit and the data derived from the diffraction pattern were compared with ASTM data, and are presented in Table 2.

The chemical compositions of the codeposits were also estimated with the help of a Perkin-Elmer atomic absorption spectrophotometer (AAS, Model 380) by chemical stripping of the deposits with acid solutions.

*Table 2. XRD data obtained on Ni–Mo–Fe electrolytic codeposits on mild steel*

| *Measured d/nm* | *Standard value d/nm (ASTM)* | $I/I_0$ | *Phase* |
|---|---|---|---|
| 0.203 | 0.203 | 100 | Ni, $\alpha$-Fe |
| 0.223 | 0.225 | 89 | Mo |
| 0.134 | 0.133 | 50 | Ni |
| 0.129 | 0.127 | 34 | Mo |
| 0.117 | 0.120 | 30 | Fe |
| 0.157 | 0.164 | 23 | Mo |
| 0.143 | 0.140 | 19 | Fe |
| 0.265 | 0.272 | 40 | |
| 0.143 | 0.140 | 5 | $MoO_3$ |

### 2.3. *Current–potential relationships*

The deposited electrodes were tested for the evaluation of electrochemical parameters, by exposing a geometric area of 8.0 cm$^2$. The experiments were carried out in a three-compartment stainless steel cell under galvanostatic steady state conditions. Two nickel plates with sufficiently large area, contained in nylon bags, were used as auxiliary electrodes. As reference, a Hg/HgO, $OH^-$ electrode in the working solution, linked to the main compartment via a Luggin capillary, was used. The potentiodynamic experiments were carried out using a PAR Model 370 Electrochemistry System. Alkaline solution (6 M) was prepared from analytical grade KOH pellets in triple distilled water and was pre-electrolysed for more than 48 h at 100 mA cm$^{-2}$ between two platinum electrodes in order to eliminate the electroactive impurities. The working electrodes were precathodized at 1 mA cm$^{-2}$ for 30 min at room temperature. The open circuit potentials (o.c.p.) were measured after 60 min at equilibrium conditions. The galvanostatic steady state potential values measured

as a function of applied current densities were compensated for the *IR* components and used to construct the Tafel plots. The *IR* components were measured using an interruptor method.

### 2.4. *Reverse potential cycling (RPC) tests*

An accelerated experiment [10] was adapted to assess the stability of the present codeposit cathodes. The precathodized electrode was scanned potentiodynamically to 200 mV, positive with respect to the reversible hydrogen electrode potential (RHEP) at $0.5\,mV\,s^{-1}$. The scan was then reversed at the same rate to 100 mV, negative with respect to RHEP. This cycling was continued until a significant change in the behaviour was observed. A plot of the limiting anodic oxidation current density at $-0.85$ V as a function of the number of cycles was constructed.

### 2.5. *Time variation analysis*

Time variation analysis was carried out in a three-compartment 10 $dm^3$ capacity stainless steel tank containing 8 $dm^3$ of the same alkaline solution. The time variation effect of the cathode potential was studied by applying a constant cathodic current density for a long time with periodic replenishment of the electrolyte with triple distilled water to the original volume to balance the water lost on electrolysis. The accelerated life tests were carried out by suddenly raising the current density value to a specific value at regular time intervals of five days and monitoring the shift in the potential with time for 5 h. The simulation experiments were performed by subjecting the cathodes to common industrial conditions. The circuit was interrupted over time intervals ranging from 5 to 10 days and again closed to test the effect of such severe but common incidents on the cathode potential in industrial water electrolysis.

### 2.6. *Thermal activation procedures*

As inclusion codeposits are likely in any electrolytic codeposition involving transition metals, such as Mo and W [11], the thermal activation of such systems at high temperatures in a hydrogen atmosphere was found [12] to improve their catalytic properties. Hence the deposited samples were laid down in an alumina tube, placed inside a glove box made of stainless steel and subjected to thermal activation in a hydrogen atmosphere in the temperature range 573 to 1073 K for various times. The effect of this treatment on the catalytic properties was investigated by applying a constant cathodic current density, $300\,mA\,cm^{-2}$ at typical electrolyser operation conditions for 6 h and measuring the cathode potential at the end of this period. The data presented in Table 5 were obtained by testing three identical test pieces in each category; the values were not compensated for *IR* components.


Fig. 1. SEM for Ni–Mo–Fe ternary codeposit surface as deposited.

## 3. Results and discussion

### 3.1. *Physical characteristics of the codeposits*

The feasibility of codeposition of metals like Mo, W, Co, Fe, Zn and Cr along with Ni is well established [13–17] although Mo cannot be electrodeposited from aqueous solutions [18] as such. The thickness of the coatings ranged from 4.0 to 12 $\mu$m for the present group of ternary codeposits. The adhesion of the codeposits to the substrates was very good.

The scanning electron micrographs of the Ni–Mo–Fe, Ni–Mo–Cu and Ni–Mo–Zn electrolytic ternary codeposit surfaces as deposited are shown in Figs 1, 2 and 3. These micrographs show that the surfaces have, in general, fine grained microstructures. Further, they show evidence of stress and fine cracks.

### 3.2. *Chemical compositions of the ternary codeposits*

The EPMA spectra exhibited a regular distribution pattern of the metals concerned in each of the codeposits. The relative chemical compositions of the ternary codeposits were found to be 70% Ni, 15% Mo, 15% Fe for Ni–Mo–Fe; 74% Ni, 14% Mo, 11% Cu for Ni–Mo–Cu; 55% Ni, 10% Mo, 32% Zn for Ni–Mo–Zn; 60% Ni, 18% Mo, 22% W for Ni–Mo–W; 55% Ni, 10% Mo, 34% Co for Ni–Mo–Co; and 85% Ni, 10% Mo, 12% Cr for Ni–Mo–Cr by gram atomic weight. The XRD pattern obtained for Ni–Mo–Fe was analysed; the phases present in the Ni–Mo–Fe codeposit also include $MoO_3$ as inclusion codeposit.

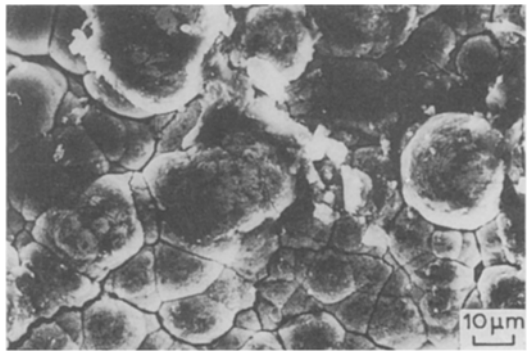


Fig. 2. SEM for Ni–Mo–Cu ternary codeposit surface as deposited.


Fig. 3. SEM for Ni–Mo–Zn ternary codeposit surface as deposited.

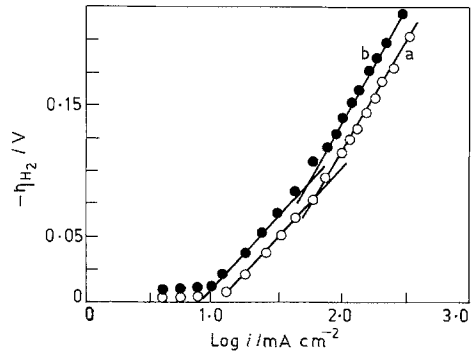


Fig. 4. Tafel plots of the h.e.r. on Ni–Mo–Fe ternary electrodeposits (a) at 353 K (b) at 303 K in 6 M KOH.

### 3.3. *Electrochemical behaviour of the ternary codeposit cathodes*

The reversible o.c.p. values measured on these cathodes ranged from −860 to −960 mV as a function of temperature. These data are presented in Table 3. It becomes evident that the influence of temperature on these values is very significant. This suggests that the adsorption of hydrogen formed during the precathodization step on the cathode surfaces is influenced significantly by the temperature, resulting in changes in the open-circuit potential values.

The Tafel plot for the h.e.r. obtained on the Ni–Mo–Fe ternary codeposit cathode is shown in Fig. 4. Similar plots were also obtained on Ni–Mo–Cu, Ni–Mo–Zn, Ni–Mo–Co, Ni–Mo–W and Ni–Mo–Cr codeposit cathodes (figures not shown). It was noted that dual Tafel slopes exist in all the plots. The apparent values of Tafel slopes and equilibrium exchange current density were derived from these. Arrhenius plots were made both at low and high polarization conditions, as shown in Figs 5 and 6, to calculate the apparent energy of activation values. The h.e.r. parameters obtained on these cathodes are presented in Table 4. The following points can be made from these data:

1. All the ternary codeposit cathodes, based on transition metals considered here, exhibited electrocatalytic activity towards the h.e.r.
2. The cathodic contribution to the electrolyser voltage can be reduced by 0.3 V under typical industrial conditions by employing the Ni–Mo–Fe codeposit cathode in the place of conventional mild steel cathodes.
3. The Tafel slope values for the codeposits Ni–Mo–Cu, Ni–Mo–Zn, Ni–Mo–W, Ni–Mo–Co and Ni–Mo–Cr under low polarization conditions ($i$ < 50 mA cm$^{-2}$) range from 24 to 32 mV dec$^{-1}$. The value for Ni–Mo–Fe under these conditions is 115 mV dec$^{-1}$. Under high polarization conditions, the values range from 116 to 180 mV dec$^{-1}$. This wide variation arises from the fact that, as the present group of closely related cathodes are subjected to high current densities, the influence of

*Table 3. The reversible o.c.p. values of electrolytic ternary codeposit cathodes*

| *Sl. No.* | *Codeposit* | *Potential/mV against Hg/HgO, OH⁻ (6 M)* | *Temperature /K* |
|---|---|---|---|
| 1. | Ni–Mo–Fe | −957 | 303 |
| | | −941 | 318 |
| | | −924 | 333 |
| | | −912 | 353 |
| 2. | Ni–Mo–Cu | −952 | 305 |
| | | −943 | 318 |
| | | −927 | 333 |
| | | −914 | 353 |
| 3. | Ni–Mo–Zn (after leaching Zn in KOH) | −955 | 305 |
| | | −940 | 318 |
| | | −924 | 333 |
| | | −907 | 353 |
| 4. | Ni–Mo–W | −941 | 305 |
| | | −921 | 318 |
| | | −909 | 333 |
| | | −902 | 353 |
| 5. | Ni–Mo–Co | −917 | 305 |
| | | −900 | 318 |
| | | −882 | 333 |
| | | −860 | 353 |
| 6. | Ni–Mo–Cr | −894 | 305 |
| | | −871 | 318 |
| | | −862 | 333 |
| | | −855 | 353 |
| 7. | Ni-plated mild steel | −901 | 305 |
| | | −871 | 318 |
| | | −852 | 333 |
| | | −840 | 353 |

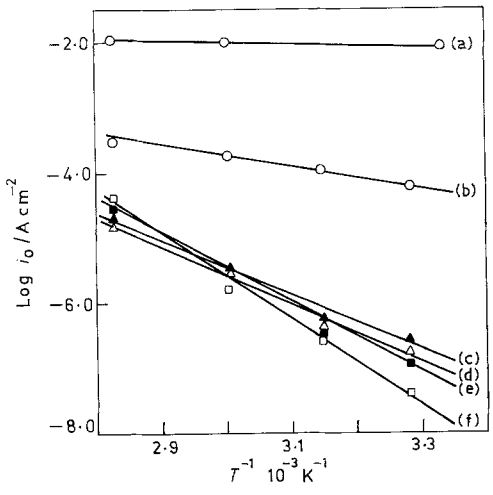


Fig. 5. Arrhenius plots of the h.e.r. on ternary codeposits, under low polarization conditions: (a) Ni–Mo–Fe; (b) Ni–Mo–Cu; (c) Ni–Mo–Zn; (d) Ni–Mo–Co; (e) Ni–Mo–W; (f) Ni–Mo–Cr.

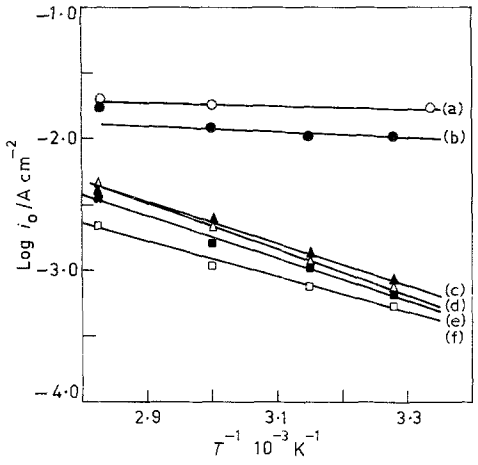


Fig. 6. Arrhenius plots of the h.e.r. on ternary codeposits, under high polarization conditions: (a) Ni–Mo–Fe; (b) Ni–Mo–Cu; (c) Ni–Mo–W; (d) Ni–Mo–Zn; (e) Ni–Mo–Co; (f) Ni–Mo–Cr.

the adsorption effects of the evolved hydrogen predominates and deviation from Tafel linearity occurs. 4. The apparent energy of activation for the h.e.r. on these codeposit cathodes are very low in magnitude compared with that for pure nickel and many other systems [15, 19].

The magnitude of the Tafel parameters (24 to 32 mV dec$^{-1}$) obtained on Ni–Mo–Cu, Ni–Mo–Zn, Ni–Mo–W, Ni–Mo–Co and Ni–Mo–Cr ternary codeposit cathodes under low polarization conditions ($i < 50$ mA cm$^{-2}$) agree well with the values of other authors on transition metal-based coatings, that is on Ni–Fe electrodeposits [19], Ni–Mo thermal deposits [20] and Ni–Mo–Cd electrolytic codeposit cathodes [21, 22]. The Tafel slope value on the Ni–Mo–Fe codeposit cathode (115 mV dec$^{-1}$) is not in agreement with the results of similar electrodes, for example, Ni–Mo–Cd cathodes [21, 22]. The very low values reported by these authors (30 to 38 mV dec$^{-1}$) were estimated in the current density region from 0.01 mA cm$^{-2}$ to 30 mA cm$^{-2}$. However, in view of the common practical alkaline water electrolysis conditions, namely 300 mA cm$^{-2}$ > $i$ > 10 mA cm$^{-2}$, in the present work the Tafel parameters were obtained under these conditions. The values obtained under high polarization conditions ($i > 100$ mA cm$^{-2}$) vary significantly among the ternary codeposit cathodes. The $E$ values suggest that the present results reflect changes in the surface coverage of the adsorbed hydrogen on different codeposit cathodes. Thus, no correlation exists among the d-band structures of the constituent metals and the $\Delta E$ values.

### 3.4. *Catalytic activation effects*

As transition metals such as Ni, Fe, Co and W are prone to oxidation, the effect of thermal pretreatment of these ternary codeposits in a hydrogen atmosphere on the catalytic activities for the cathodic hydrogen evolution was investigated. The results are presented in Table 5 and the following points are obvious: (a) that, in general, the hydrogen overpotential values are lower in the case of activated surfaces when compared with unactivated surfaces; (b) that a reduction of 50 mV in the hydrogen overpotential values is possible under the optimum treatment conditions, namely, thermal activation at 1073 K for 5 h in a hydrogen atmosphere on a Ni–Mo–Fe cathode; and (c) that the treatment at higher temperatures, or for a long time at the optimum temperature, does not help much (results not shown in Table 5).

### 3.5. *Life tests by simulation experiments*

The time variation effects of the cathode potentials for the Ni–Mo–Fe, Ni–Mo–Zn and Ni–Mo–Cu codeposit cathodes on continuous operation in 6 M KOH at 300 mA cm$^{-2}$ and 353 K is shown in Fig. 7. The results of accelerated life tests carried out on the Ni–Mo–Fe cathode indicated that the variation in the cathode potential is 35 mV over a period of 60 days at 600 mA cm$^{-2}$ and 353 K. The results obtained on the other codeposit cathodes indicated a variation of 60 to 80 mV over a period of about 10 days. This means that the electrochemical behaviour of the codeposits was modified significantly under these accelerated test conditions involving vigorous gas evolution, which may arise accidentally in commercial cells. The simulation experiments indicated a jump of 75 mV in the o.c.p. value over an interruption duration of 15 days on the Ni–Mo–Fe cathode, which means that hydrogen bubbles become detached from the surface slowly with time. The results of simulation experiments on other codeposit cathodes under identical conditions indicated wide variation (e.g., 105 mV on Ni–Mo–Cu; 126 mV on Ni–Mo–Zn; 155 mV on Ni–Mo–W; 150 mV on Ni–Mo–Co; 196 mV on Ni–Mo–Cr) in the o.c.p.

*Table 4. Electrochemical parameters for the h.e.r. on different cathode materials*

| *S. No.* | *Codeposit* | *Temp./K* | *b/mV dec$^{-1}$* | | *Energy of activation/kJ mol$^{-1}$* | | *$-\eta(H_2)$ at 300 mA cm$^{-2}$* |
|---|---|---|---|---|---|---|---|
| | | | *at $i$ < 50/ mA cm$^{-2}$* | *at $i$ > 50/ mA cm$^{-2}$* | *at low $\eta$* | *at high $\eta$* | |
| 1. | Ni–Mo–Fe | 353 | 115 | 165 | 4.78 | 4.308 | 187 |
| 2. | Ni–Mo–Cu | 353 | 28 | 180 | 44.6 | 9.57 | 190 |
| 3. | Ni–Mo–Zn | 353 | 24 | 116 | 81.37 | 30.64 | 220 |
| 4. | Ni–Mo–W | 353 | 28 | 150 | 86.16 | 26.42 | 265 |
| 5. | Ni–Mo–Co | 353 | 26 | 140 | 76.59 | 26.42 | 270 |
| 6. | Ni–Mo–Cr | 353 | 32 | 165 | 114.8 | 49.78 | 350 |
| 7. | Base mild steel | 353 | 135 | 125 | 59.8 | 68.1 | 540 |

*Table 5. Effects of thermal activation in hydrogen atmosphere on the catalytic activities of different cathodes*

| S. No. | Codeposit | Temp./K | Duration/h | $-E^*_{300}$ at 353 K/mV |
|---|---|---|---|---|
| 1. | Ni-Mo-Fe | 573 | 5 | 1150 |
| | | 773 | 5 | 1145 |
| | | 1073 | 5 | 1086 |
| | | 1073 | 10 | 1080 |
| 2. | Ni-Mo-Cu | 1073 | 5 | 1110 |
| | | 1073 | 10 | 1100 |
| 3. | Ni-Mo-Zn | 1073 | 5 | 1179 |
| | | 1073 | 10 | 1169 |
| 4. | Ni-Mo-W | 1073 | 5 | 1205 |
| | | 1073 | 10 | 1200 |
| 5. | Ni-Mo-Co | 1073 | 5 | 1220 |
| | | 1073 | 10 | 1205 |
| 6. | Ni-Mo-Cr | 1073 | 5 | 1295 |
| | | 1073 | 10 | 1285 |

* $E$ values are not compensated for $IR$ and obtained at 300 mA cm$^{-2}$

values. The interesting point here is that the original potential values were again established by subjecting the cathodes to a current density of 0.1 $\mu$A cm$^{-2}$ for some time (60 min). From this, it is concluded that the open circuit stability can be conserved by applying a negligibly small cathodic current density while they are not in use [2].

### 3.6. *Reverse potential cycling (RPC) tests*

The behaviour of Ni-Mo-Fe codeposit cathode with respect to the hydrogen oxidation potential is illustrated from the plot of anodic limiting oxidation currents observed in the RPC experiments against the number of cycles in Fig. 8. The currents observed on other codeposit cathodes were much less when compared with that of Ni-Mo-Fe (not shown in figure). This indicates stronger hydrogen adsorption on the Ni-Mo-Fe codeposit, leading to higher oxidation currents. As the magnitude of these currents is not sufficient [9] to represent the oxidation of the electrode and does not vary much on repeated cycling, it is obvious that these currents represent the oxidation of the dissolved and adsorbed hydrogen on the electrode surface. Since it is unlikely that a cathode in a unipolar water electrolyser would ever experience a potential as high as this, this test is sufficient to evaluate their suitability

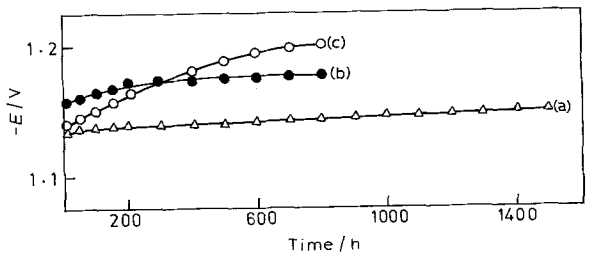


Fig. 7. Time variation effects of the cathode potentials at 300 mA cm$^{-2}$ and at 353 K in 6 M KOH (a) Ni-Mo-Fe; (b) Ni-Mo-Zn; (c) Ni-Mo-Cu.

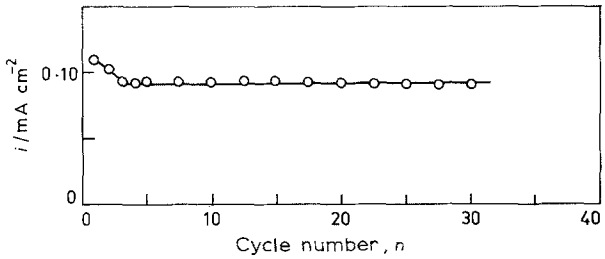


Fig. 8. Plot of anodic limiting oxidation currents observed in the reverse potential cycling experiments against the number of cycles in 6 M KOH at 301 K and at −0.85 V against Hg/HgO,OH$^-$ on Ni-Mo-Fe.

under open circuit conditions. The results reported in this work do not agree with the result of other similar work [9], possibly owing to the very short delay of the cathode at +200 mV to the open circuit potential.

## 4. Conclusions

From these results we conclude that Ni-Mo-Fe electrolytic ternary codeposits, obtained from an alkaline citrate bath, on mild steel substrates are effective and promising cathodes for energy efficient alkaline water electrolysis. The use of this three component coating in industrial cells demands very high stability (periods ranging from 2 to 3 years) on continuous operation. The results of a few simulation experiments carried out on a Ni-Mo-Fe codeposit cathode with a view to assess its practical utility will form the subject of our next communication.

## Acknowledgement

The authors thank the Director of CECRI, Karaikudi, for his permission to publish this paper.

## References

[1] I. Arul Raj and K. I. Vasu, *J. Appl. Electrochem.* **20** (1990) 32.
[2] I. Arul Raj and V. K. Venkatesan, *Int. J. Hydrogen Energy* **13** (1988) 215.
[3] *Idem., Trans. SAEST (India)* **22** (1987) 189.
[4] M. M. Jaksic, *Electrochim. Acta* **29** (1984) 1539.
[5] L. Vracar and B. E. Conway, *ibid.* **15** (1990) 701.
[6] E. Potvin, H. Menard, J. M. Lalancette and L. Brosard, *J. Appl. Electrochem.* **20** (1990) 252.
[7] J. Divesek, P. Malinowski, J. Mergel and H. Schmitz, *Int. J. Hydrogen Energy* **13** (1988) 141.
[8] M. R. Gennero de Chialvo and A. C. Chialvo, *Electrochim. Acta* **33** (1988) 825.
[9] D. E. Brown, M. N. Mahmood, M. C. M. Man and A. K. Turner, *ibid,* **29** (1984) 1551.
[10] M. B. Janjua and R. L. Le Roy, *Int. J. Hydrogen Energy* **10** (1985) 11.
[11] A. Brenner, *in* 'Electrodeposition of Alloys, Principles and Practice', Vol. 2, Academic Press, New York (1963) p. 430.
[12] H. Wendt and V. Plzak, *Electrochim. Acta* **28** (1983) 27.
[13] E. Beltowska-Lehman and K. Vu Quang, *Surf. Coat. Technol.* **12** (1986) 75.
[14] C. Karwas and T. Hepel, *J. Electrochem. Soc.* **135** (1988) 839.
[15] D. E. Hall, *ibid.* **128** (1981) 740.
[16] P. W. T. Lu and S. Srinivasan, *ibid.* **125** (1978) 265.
[17] B. Tereszko, A. Risenkampf and K. Vu Quang, *Surf. Coat. Technol.* **12** (1981) 301.
[18] A. T. Wasko, 'Electrochimia molibdina i wolframa', Izd.

Naukowa Dunka, Kiev (1977).
[19] E. R. Gonzales, L. A. Avaca, A. Carubelli, A. A. Tanaka and G. Tremiliosi-Filho, *Int. J. Hydrogen Energy* **9** (1984) 689.
[20] D. E. Brown, M. N. Mahmood, A. K. Turner, S. M. Hall and P. O. Fogarty. *ibid.* **7** (1982) 405.
[21] B. E. Conway, H. Angerstein-Kozlowska, M. A. Sattar and B. V. Tilak, *J. Electrochem. Soc.* **130** (1983) 1825.
[22] B. E. Conway and L. Bai, *J. Chem. Soc., Faraday Trans., 1*, **81** (1985) 1841.